Electric Power Systems Research 212 (2022) 108293

Contents lists available at ScienceDirect

Electric Power Systems Research

journal homepage: www.elsevier.com/locate/epsr

Analytical approach for adequacy assessment of cyber–physical multi-microgrid distribution systems with distributed generation

Mostafa Barani *, Vijay Venu Vadlamudi

Department of Electric Power Engineering, Norwegian University of Science and Technology (NTNU), Trondheim, Norway

ARTICLE INFO

Keywords:
Adequacy
Analytical method
Cyber–physical distribution system
Multi-microgrid system
Renewable energy resources

ABSTRACT

In recent years, there has been a marked increase in the deployment of information and communication technologies (ICTs) in power systems. ICTs impart a cyber-physical nature to power systems, and though they improve the power system performance in various respects, they themselves are prone to random failures. With even more extensive penetration of ICTs expected to strongly characterise the future power systems, it is imperative to systematically study the impact of failures in cyber-physical power systems on the adequacy of power systems. With this as backdrop, the paper presents a novel analytical approach to study the impact of failure of various control layers and the cyber links between them on the adequacy of multi-microgrid distribution systems consisting of distributed generation resources such as wind and solar units. The main adequacy index of interest is Expected Energy Not Served, based on which the interruption costs can be computed. A case study is presented where the developed methodology is applied to a multi-microgrid distribution system where four different operation modes are realisable—normal, joint, islanding, and shutdown modes. The results are validated against those of a recently developed Monte Carlo simulation approach.

1. Introduction

1.1. Motivation and background knowledge

The concepts of Microgrid (MG) and Multi-Microgrid (MMG) systems have been well developed in recent years, especially to facilitate the vast scale integration of Distributed Energy Resources (DERs) and active loads in the power system [1–3]. Successful implementation of these systems is made possible through advanced information and communication technologies (ICTs), which enhance the functionality of distribution networks in different aspects, viz., automation of system control, system monitoring, peer-to-peer communication, and data gathering & processing [4]. The resulting Cyber-Physical Distribution Systems (CPDS) (or to be more precise, Cyber-Physical Multi-Microgrid (CPMMG) systems) considerably improve the power system performance in various aspects. However, cyber systems in practice are not failure-free, and the impact of these random failures in CPMMG system on the adequacy aspect of their reliability cannot be neglected, and needs to be studied systematically. With this motivation in place, the objective of the paper is to present a novel approach to assess the adequacy of a CPDS consisting of multiple MGs and distributed generation resources such as wind and solar units.

There are two types of impacts—direct & indirect—that a failure in cyber component, w.r.t. its function, exerts on power system [4]. There are generally a number of methods for analysing these impacts [5]. The literature in this field, by incorporating more comprehensive cyber structure and utilising different methods to model the effects of their failure, has gradually evolved for distribution networks and isolated MGs during the last decade. To name a few, Falahati et al., in one of the earliest attempts, proposed two methods for incorporating direct and indirect impact of cyber failures on overall adequacy of a power system, respectively [4,6]; Liu et al. recently proposed a simulation-based method [7] and an analytical approach [8] for reliability evaluation of CPDS. There are also several studies on the reliability of isolated MGs, notable among them being the sequential Monte Carlo method developed by Wang et al. [9] for the operational reliability of MGs.

1.2. Proposed methodology: Outline & contribution

With respect to the increasing penetration of DERs into the distribution networks, their transformation to the MMG distribution networks is plausible [10]. This transformation changes the cyber infrastructure and requires additional control layers [11]. The authors of the

* Corresponding author.
E-mail addresses: mostafa.barani@ntnu.no (M. Barani), vijay.vadlamudi@ntnu.no (V.V. Vadlamudi).

https://doi.org/10.1016/j.epsr.2022.108293
Received 3 October 2021; Received in revised form 21 April 2022; Accepted 2 July 2022
Available online 18 July 2022

Table 1
Types of interdependencies and the consequence of cyber failures considered in this study.

Failure	Impact	Consequence
DMS	Direct	Shifting of all MGs to the islanding mode
Cyber link between DMS and upstream network	Direct	Disconnection of distribution system from upstream network
MGCC	Direct	Shutdown of the related MG
Cyber link between an MGCC and the DMS	Direct	Shift of the related MG to islanding mode
All cyber links to/from MGCC	Direct	Shutdown of the related MG
CBCs or all their cyber links	Indirect	Inaccessibility of circuit breaker (mis-operation mode)
MCs or their connection to the corresponding MGCC	Direct	Outage of the corresponding DG
LCs or their connection to the corresponding MGCC	Indirect	Uncontrollable load point

current paper recently developed an approach based on Monte Carlo simulation (MCS) for identifying and incorporating the impact of these additional control layers, and assessed the adequacy of a grid-connected MG [11]; this study has been further extended to include MMG considerations [12]. On the one hand, the reliability assessment methods based on MCS are effective and can include the detail of the system as desired. On the other hand, they are relatively time-consuming. Therefore, to accelerate the procedure, the proposed systematic approach in this paper focuses on a novel analytical methodology, encompassing state enumeration, classification of components, and probability theory, for the adequacy assessment of a CPMMG system as an integrated system including non-dispatchable renewable generation resources (wind and solar units) and dispatchable generation resources (small scale thermal units). It will be shown that the proposed approach is a viable alternative to the time-consuming MCS-based approach. In order to validate the proposed methodology, the results are compared with those obtained using MCS. In addition, as will be explained, the ownership of MGs in an MMG is important in adequacy assessment. We have recently proposed two indices to capture this impact of ownership [11]. The model in this paper has also been tailored to calculate these indices. Therefore, the model is applicable for CPMMGs with either *single* or *multiple self-interested* owners.

1.3. Organisation of the paper

The rest of the paper is organised as follows. Section 2 explains the CPMMG systems and the direct & indirect impacts of cyber failures. Section 3 elaborates the procedure to acquire the probability of being in different operation modes. The operation of the system in various operation modes is modelled in Section 4. Section 5 shows the procedure for calculating the adequacy indices. The result of case studies are given and analysed in Section 6, and the concluding remarks are finally provided in Section 7.

2. Cyber-physical multi-microgrid systems

A multi-microgrid distribution system can have different structures w.r.t. the arrangement of MGs in the system. Fig. 1 shows a sample CPMMG, whose structure is more general; as such, the proposed methodology can be adapted to any other specific structure of the MMG distribution networks. The impact—direct or indirect—of a failure of a cyber component depends on the functions and logic that are defined for that cyber component. In this regard, in order to determine these dependencies, one should first determine the logic and design of the control systems, which can then be used to define the dependencies of the power system on the cyber system. For instance, the MG with centralised control system cannot operate when its centralised control system fails. As another example, the consequence of failure of protection system depends on its design. This paper considers a centralised control system at both layers, viz., MMG and MGs. Accordingly, the impact of malfunction of different cyber components assumed in this study, taken from [12], is listed in Table 1. For the sake of clarity, note that a cyber route in this paper refers to a single communication route between two cyber components, and a cyber link refers to all communication routes between two components.

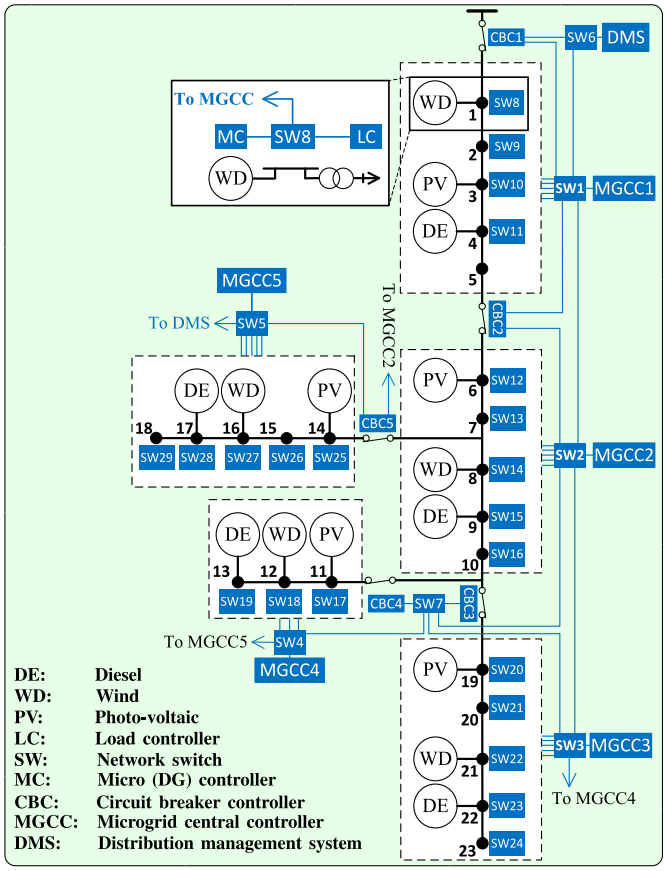

Fig. 1. Schematic diagram of CPMMG under study.

3. Determining the operation mode of MGs

A single MG in an MMG system must be properly designed to operate in different operation modes. An MG, most of the time, is in normal operation mode, whereby it is connected to the upstream network. Some events might force an MG to shift to island, joint, and shutdown modes. In joint operation (JO) mode some MGs are connected to each other but separated from the upstream network. Assume the simple three-microgrid system in Fig. 2; it includes three possible combinations for joint operation mode. MG #1 exists in all these combinations and can be in total in six operation modes: 1) normal, 2) shutdown, 3) islanding 4) JO #1 {MG1, MG2, MG3}, 5) JO #2 {MG1, MG2}, and 6) JO #3 {MG1, MG3}. This section elaborates the procedure to derive the occurrence probability of various operation modes in a CPMMG.

3.1. Step 1: Aggregation of components

The components whose failure exert an identical impact on the system are aggregated as one component based on the concept of series

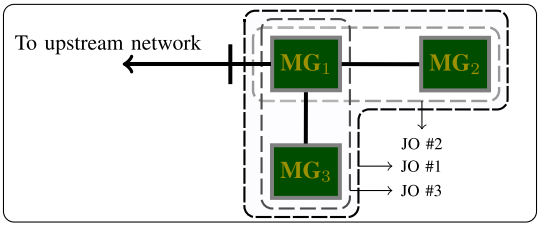

Fig. 2. Various possible joint operation modes for a sample MMG. Among these, in this configuration, only JO #1 can occur by a single failure; Since A ≫ U for all components in CPPMG, the occurrence probability of JO #1 is then obviously much higher than that of JO #2 & JO #3.

and parallel systems. These components in Fig. 1 are the power lines in the same zones w.r.t. the power switches. In the cyber system, the contiguous components without other lateral connections can be grouped as one component. For example, the DMS and MGCCs and their associated fibre optic connections. It is also possible to aggregate the cyber & power components. As assumed in Table 1, the cyber link between the DMS and the upstream network is necessary for normal operation of the system. In this regard, the impact of failure of the upstream network is the same as the impact of failure of the cyber link to the upstream network, and thus the upstream network and the cyber link to the upstream network can be grouped together as one component. The availability and unavailability for each set of aggregated components, $\mathcal{O}^{\text{ACO}}$, are $\prod_{e\in\mathcal{O}^{\text{ACO}}} A_e$ and $1-\prod_{e\in\mathcal{O}^{\text{ACO}}} A_e$, respectively.

3.2. Step 2: Classification of the components

In order to decrease the size of the state space of the State Enumeration Method (SEM), the proposed methodology classifies the components of the CPMMG into the following categories:

(1) Critical components whose single failure changes the operation mode of at least one of the MGs together with the fibre optics connecting MGCCs, and MGCCs & DMS.
(2) Cyber components that affect the accessibility of the power switches except those in the first category.
(3) Components whose failure may result in outage of load points, uncontrollable load points, and outage of DGs except those in the first category.

This classification drastically decreases the size of state space generated by the SEM, which is specially effective for larger systems. However, depending on the cyber structure, the classification may yield absolutely negligible approximations. This classification is further discussed in Section 3.5.1. In the rest of the paper, the aforementioned categorised components are referred to as the first, second, and third category of components, respectively. The first two categories of components are taken into account to calculate the occurrence probability of various operation modes.

3.3. Step 3: Applying state enumeration method to the first category of the components

In this step, SEM is applied to the first category of the components. The total number of states is $2^{n^{g1}}$; where n^{g1} is the number of the components in the first category. Most of the analytical approaches proposed for the adequacy assessment of distribution networks in the literature consider a first-order (N−1 criteria) contingency. As it will be shown in the result, this assumption is mostly acceptable, since the single contingencies are the main cause of load interruption in the system. However, using SEM, we can easily calculate the impact of higher order of contingencies to see whether it is required to consider a higher order of contingency. A threshold for filtering the states can then be used for eliminating the insignificant states. Each state s generated by SEM includes the state of all individual components—working or failed—of the first category of the components and its associated occurrence probability, which is calculated as follows:

$$\rho_s^{\text{SEM}} = \prod_{e_1\in\mathcal{O}_s^{\text{A}}} A_{e_1} \times \prod_{e_2\in\mathcal{O}_s^{\text{U}}} U_{e_2}. \tag{1}$$

$\mathcal{O}_s^{\text{A}}$: Set of available components in state s.

$\mathcal{O}_s^{\text{U}}$: Set of unavailable components in state s.

A_e: Availability of component e.

U_e: Unavailability of component e.

3.4. Step 4: Analysing the states obtained by SEM and determining the MGs in islanding and shutdown modes

In this step, each of the states that has passed the SEM filter is analysed, and based on the failed cyber and power components the MGs in islanding and shutdown modes, and failed power switches are determined. For instance, the failure of MGCC_1 or any power distribution line inside MG #1 results in the shutdown of the associated MG.

In order to identify the islanded MGs, it is required to determine the availability of the cyber links between the MGs and the DMS. To determine the cyber links, the method explained in [11] is used, where a cyber link is defined by a *structure function* in the form of minimal sum-of-products. The minimal path sets required in this method can be efficiently determined using the graph of the fully operational cyber system. However, depending on the cyber topology, some components in these path sets may not be in the first category of the components (Let $\mathcal{H}$ be the set of these components, and let internal cyber routes refer to the path sets that include any of the components in $\mathcal{H}$); therefore, their states are not determined in the states generated by SEM. As this only occurs when there is a redundancy in the cyber links, it can be assumed that these components are available. The availability of the cyber links can be determined accordingly. The approximation is completely negligible. Nonetheless, the impact of failure of internal routes may be considered when there is a star topology between the MGCCs and the DMS, and just for those states (output of SEM) where the only failed component is the Fibre Optic (FO) between the MGCC and the DMS. For this case, the components inside the set $\mathcal{H}$ whose single failure results in the failure of all the internal routes are determined. Let $\mathcal{K}$ be the set of these components. The unavailability of all internal routes in this case is approximately calculated as $\zeta = \sum_{e_1\in\mathcal{K}} U_{e_1} \prod_{e_2\in\mathcal{H}-e1} A_{e_2}$. The state s under study is then split into two states with the probability of $\rho_s^{\text{SEM}} \times \zeta$ and $\rho_s^{\text{SEM}} \times (1-\zeta)$, where in the first state, the associated MG is marked as islanded. Assume that there is a star topology between the MGCCs and the DMS in Fig. 1. In this case, the components inside the set $\mathcal{H}$ for MGs #2-4 include SW_7 and the FOs that connect it to the MGCCs. The set $\mathcal{K}$ for MG #2, for example, includes SW_7 and the FO that connects it to the MGCC_2. The implementation of the outlined procedure, though not exact, is generally easier for complex cyber structures; in the case considered here (Fig. 1), an exact and straight forward equation for ζ could be derived.

3.5. Step 5: Indirect impact of the power switch controllers

3.5.1. Probability of proper operation of switches

A faulty MG or an MG that should shift to shutdown or island modes requires the operation of power switches that surround it. If any of these switches are not accessible, the failure extends to the

neighbouring MGs. In this regard, it is required to calculate the probability of accessibility of the involved power switches. The impact of the failure of cyber components on the accessibility of the power switches depends on the design of their operation. For example, in a differential protection, the controllers of the power switches at both ends together with the cyber link between them are necessary for the proper operation of the protection system of a section. In this study, the DMS and MGCCs are responsible for the operation of the power switches. Accordingly, the availability of its controller is calculated based on the logic below, provided that the power switch itself is working.

- The power switch is accessible if the related Circuit Breaker Controller (CBC) and its cyber link to one of the neighbouring MGCCs, or the DMS are available.

Consider the circuit breaker between MG #1 and MG #2 in Fig. 1. The goal is to find the accessibility of its CBC, i.e., CBC_2. According to the above logic, $MGCC_1$, $MGCC_2$, and the DMS can provide command signal for this CBC. Fig. 3.a depicts the cyber components that affect the accessibility of this switch. The state of the components highlighted with blue colour are known (output of SEM) in the state under study. ACOs are aggregated components that have been reduced to one component in step 1. The accessibility of this power switch is calculated as follows:

$$A_{CB_2} = \left[1 - (1 - X_{P_1}(s) \times A_{FO_3}) \times (1 - X_{P_2}(s) \times A_{FO_4})\right] \times A_{CBC_2}, \quad (2)$$

where $X_{P_1(s)}$ and $X_{P_2(s)}$ are either 0 or 1 and are calculated based on the state of the components in the state s generated by SEM as follows:

$$X_*(s) = \sum_{r \in \mathcal{R}_*} \prod_{e \in \mathcal{E}_r^*} X_e(s), \quad (3)$$

where for each point *, $\{\mathcal{E}_r^*\}_{r \in R^*}$ is a family of sets, where $\mathcal{E}_r^*$ is the set of components in the r-th minimal path set between the point * and one of the corresponding controllers. As an example, for point P_1 in this structure, there are three minimal path sets to $MGCC_{\{1,2\}}$ and the DMS (corresponding controllers), and therefore, $\mathcal{R}^{P_1} = \{1, 2, 3\}$. The components inside the path sets are $\mathcal{E}_1^{P_1} = \{SW_1, ACO_2\}$, $\mathcal{E}_2^{P_1} = \{SW_{\{1,6\}}, FO_1, ACO_1\}$, and $\mathcal{E}_3^{P_1} = \{SW_{\{1,6,2\}}, FO_{\{1,2\}}, ACO_3\}$. Note that these minimal path sets can be efficiently acquired from a graph that represents the cyber system.

Now, for the same switch, assume that the connection between MGGCs and DMS forms a ring (Fig. 3.b). In this case, there are 11 path sets from P_3 to corresponding MGCCs and the DMS: $\mathcal{R}^{P_3} = \{1, 2, \ldots, 11\}$; of which one is to $MGCC_1$: $\{SW_1, ACO_2\}$; five of them are to $MGCC_2$: $\{SW_{\{1,2\}}, FO_{10}, ACO_3\}$; $\{SW_{\{1,6,5,4,3,2\}}, FO_{\{9,8,7,6,5\}}, ACO_3\}$; $\{SW_{\{1,6,5,4,7,3,2\}}, FO_{\{9,8,7,12,11,5\}}, ACO_3\}$; $\{SW_{\{1,6,5,4,7,2\}}, FO_{\{9,8,7,12,13\}}, ACO_3\}$; and $\{SW_{\{1,6,5,4,3,7,2\}}, FO_{\{9,8,7,6,11,13\}}, ACO_3\}$; and five more path sets between P_3 and the DMS. Note that the states of the components highlighted with light blue colour are not determined in the state under study, which makes an insignificant approximation. Assuming these components as available bypasses FO_6, SW_3 and FO_5; none of these are dominant components (using cut set method, these components require at least two more components to form a cut set).

Thanks to the decomposition of the components, the availability of CBC_2, in the cyber structure in Fig. 1, is independent of the availability of any other CBCs in each of the states generated by SEM. However, in some cases the probability of access to the switches are not independent of those of the other switches. For example, the availability of CBC_3 and CBC_4 are not independent due to the common network switch that they use to reach the control centres. In this case, four events are plausible, viz., (i) both accessible, (ii) only CB_3 accessible, (iii) only CB_4 accessible, and (iv) both inaccessible. Probability of each of these events is as follows:

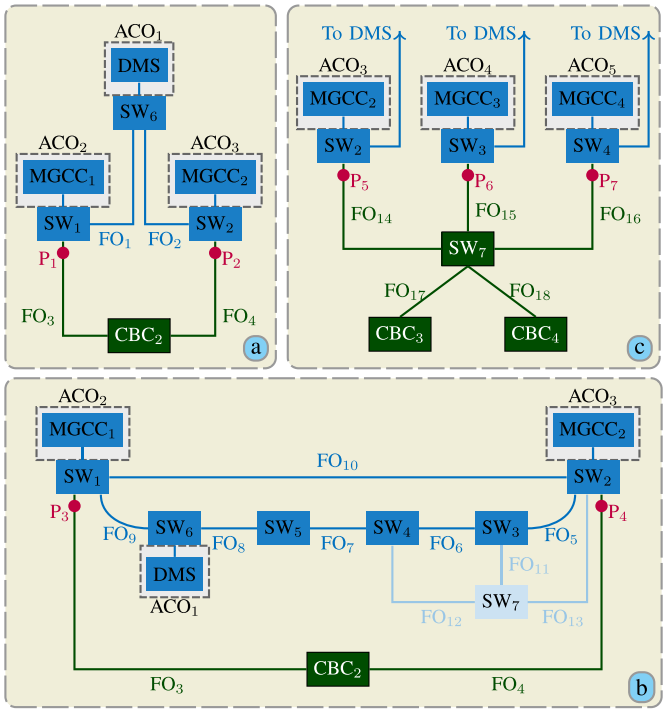

Fig. 3. Accessibility of power switches: (a) accessibility of power switch between MGCCs #1 and #2 with star connection between MGCCs and DMS; (b) accessibility of power switch between MGCCs #1 and #2 with ring topology between MGCCs and DMS; and (c) accessibility of power switches between MGCCs #2–4 with star topology between MGCCs and DMS.

$$\zeta = A_{SW_7} \times \Big[1 - (1 - X_{P_5}(s) \cdot A_{FO_{14}}) \times (1 - X_{P_6}(s) \cdot A_{FO_{15}}) \times (1 - X_{P_7}(s) \cdot A_{FO_{16}}) \Big], \quad (4)$$

$$\rho_i = \zeta \times (A_{FO_{17}} \cdot A_{CBC_3}) \times (A_{FO_{18}} \cdot A_{CBC_4}), \quad (5)$$

$$\rho_{ii} = \zeta \times (A_{FO_{17}} \cdot A_{CBC_3}) \times (1 - A_{FO_{18}} \cdot A_{CBC_4}), \quad (6)$$

$$\rho_{iii} = \zeta \times (1 - A_{FO_{17}} \cdot A_{CBC_3}) \times (A_{FO_{18}} \cdot A_{CBC_4}), \quad (7)$$

$$\rho_{iv} = 1 - (\rho_i + \rho_{ii} + \rho_{iii}). \quad (8)$$

The reliability block diagram can also be used to directly calculate ρ_{iv} as follows:

$$\rho_{iv} = 1 - \Big[\zeta \times \big[1 - (1 - A_{FO_{17}} \cdot A_{CBC_3}) \times (1 - A_{FO_{18}} \cdot A_{CBC_4})\big]\Big], \quad (9)$$

where for point *, X_* is calculated akin to the previous cases.

For some complicated structures, it is not as easy to derive a straight forward equation similar to the above cases. Consider the following example:

Assume a case where the cyber connections to the CBCs at POIs are from the closest SW at load points in Fig. 1. It is still viable to derive straight forward equations for calculating the probability of accessibility of CBCs. Now, assume that all MGs have a loop topology for connection between the SW of the MGCC and the SWs at load points. It may not be then as easy to derive straight forward equations similarly. A simple question reveals these problematic situations: *"Is there any connection between the CBC of an MG with the MGCC of a non-neighbouring MG through the components other than those in the first category?"*. If the answer is yes, one of the following alternatives may be chosen. The first alternative is the inclusion of more components in the first category. These components are all the cyber components

that connect the CBC (refer to the one in the question) to all MGCCs. In the example explained at the beginning of this paragraph, these components are all SWs and their connections among themselves and with the MGCCs in MGs #1-4. This solves the problem at the expense of increasing the state space of SEM method, which is not preferred. A second option is the removal of the problematic links. This is the easiest option, and due to the redundancy in the controllers that control the power switches, it has a completely insignificant impact on the adequacy indices. In the above explained example, this link is the connection between SW_{16} and SW_7, when we are evaluating the accessibility of CBC_2. A third option is to calculate the probability of accessibility of CBCs in such situations more accurately, using methods suitable for complex structures, such as minimal cut set method; however, due to the redundant controllers and cyber links that can provide the command signal for the CBCs, such a solution is absolutely unnecessary.

3.5.2. Updating states w.r.t. the operation of power switches

For each state s, the MGs in shutdown and islanding operation modes as well as the probability of proper operation of the power switches that surround them have already been calculated. Now, each state is split into a number of states w.r.t. the availability of the power switches. For example, if there is a failure inside MG_2 in state s, all four power switches that surround it should operate. There are in total 16 combinations for the operation of these switches. Combining the availability of controllers of these power switches, calculated in the previous step, yields the probability of each of these combinations. State s is then split into 16 states whose probabilities are obtained by multiplying the probabilities of state s and the related combination of operative switches. The shutdown MGs in new states are updated based on the non-operative switches. A threshold can also be considered here to remove the combinations with very low probability. However, to limit the approximation, its probability is added to the closest state to minimise the approximation.

3.6. Step 6: Find the occurrence probability of all modes

Each updated state now includes the following information: failed MGs, status of the power switches, status of the upstream network, and its associated probability of occurrence. The operation modes in each of the final states are derived based on the graph of the MMG as per Algorithm 1. This algorithm finds the sets of connected MGs. For instance, if only the upstream network has failed and the corresponding power switch, i.e., CB_1, is operating properly, there is only one operation mode, viz., joint operation of all MGs; therefore $S_1 = \{MG1, MG2, MG3, MG4, MG5\}$. Afterwards, the aggregated probability of being in each operation mode is calculated by summing up the associated probability of the final states that encompass that operation mode. For instance, the probability of islanding operation of MG #1 is equal to the summation of probabilities of all final states that include this operation mode. The probability of being in various modes, i.e., ρ_m^{GC}, ρ_m^{IO}, ρ_m^{SD}, ρ_j^{JO}, are now determined.

4. Operation of the system in various modes

During the islanding and joint operation modes, only the local DERs inside the MG are available for supplying the loads. In this case the level of adequacy of the MG determines the interrupted loads. First, the year is divided into time intervals with the same behaviours. The patterns of loads and renewable generation are the determinant factors in choosing the number of time intervals. Both the renewable generation and the loads have seasonal and daily patterns. In this regard, each year is categorised into 96 intervals ($\mathcal{T} = \{1, 2, \ldots, 96\}$). Each of these time intervals indicates the system behaviour in a specific hour of a specific season. Each interval then represents the system behaviour between 87 and 92 (h_t) hours depending on the season that contains it.

Algorithm 1: Find the connected MGs.

Input : Set of nodes, graph vertices, shutdown MGs, unavailable vertices*.

Output: Family set $\{S_i\}$, where S_i is the i-th set of connected zones.

```
Mark all nodes as unvisited nodes ;
Mark shutdown MGs as visited nodes;
Remove vertices that have a connection with shutdown MGs;
Remove all unavailable vertices (open power switches) ;
i ← 0 ;
while there is unvisited nodes do
    i ← i + 1;
    Choose first unvisited node;
    Find all the nodes connected to the chosen node ;
    Save the nodes in set S_i ;
    Mark all nodes in S_i as visited nodes ;
end
```

* Unavailable vertices are those with an open power switch ;

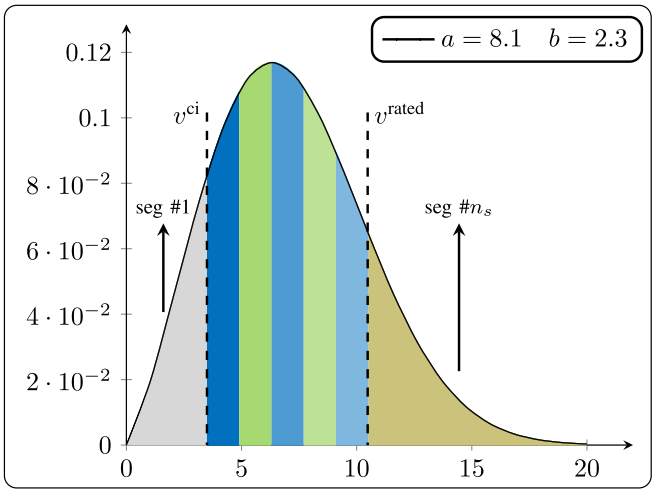

Fig. 4. Segmentation of wind speed PDF of 16th time interval. If $v > v^{co}$ is probable, another segment for $v > v^{co}$ is added and is then summed up with seg #1; $v^{ci} = 3.5$, $v^{rated} = 10.5$, $v^{co} = 25$.

4.1. Distributed energy resources

In order to model the renewable energy resources in each of the time intervals, the segmentation of Probability Density Functions (PDFs), which have been widely used in the literature [13], is applied. However, a segmentation for the PDF of the wind speed is proposed based on the characteristic of wind turbines that results in a fewer number of scenarios with the same accuracy.

The hourly PDFs are estimated using the historical data according to the method explained in [11]. Each hourly PDF is split into multiple segments. Each segment has a value and a probability of occurrence. The output generation of a wind turbine while wind is blowing at a speed less than cut-in speed or over cut-out speed is zero. In this regard, the probability of wind speed being less than cut-in speed and higher than cut-out speed can be aggregated as one scenario associated with the wind speed $v = 0$ since both have zero power production. In addition, the wind speeds between the rated and cut-out speeds result in rated output power of the wind turbines. Therefore, this interval can be considered as one scenario associated with wind speed $v = v^{rated}$. Fig. 4 indicates this segmentation method. Note that the historical wind speed data used in this study does not reach the cut-out speed; therefore, the wind speeds less than the cut-in speed are the only ones that have been considered as one segment.

Let n_t^{pv} and n_t^{w} be the number of segments of wind speed and solar radiation at time interval t; the total number of scenarios of wind

speed and solar radiation for time interval t is then $n_t^{\Omega} = n_t^{\mathrm{pv}} \times n_t^{\mathrm{w}}$. $\{\Omega_t\}_{t\in\mathcal{T}} = \{\omega \mid \omega = 1 : n_t^{\Omega}\}$ is then a family set, where Ω_t yields the set of scenarios of wind speed and solar radiation at time interval t. Note that the MGs are geographically close; therefore, only a single profile for wind and solar are considered here; therefore, the same scenario of wind speed and solar radiation is taken into account for calculating the generation of all wind and PV units. However, it should be noted that in cases where there exists more than one profile, most probably for wind speed, the correlation between these profiles must be taken into account, which is beyond the scope of this paper.

4.2. Loads

The interruption cost of various types of loads varies considerably. For example, the industrial sector is a highly sensitive sector to power interruption, and its hourly interruption cost, in one study, was estimated to be about 93 times higher than that of the residential sector [14]. In this regard, different load types—residential, commercial, and industrial—have been considered in this study. The loss of load indices are calculated accordingly.

4.3. Loss of load during island mode

For each MG m and time interval t, combining a scenario of wind and solar generation, small scale thermal unit generation, and load demands of various sectors yields one scenario of generation-load profile with its associated probability. The loads, in each scenario ω of generation-load, are supplied from the ones with the highest interruption cost to the lowest, respectively. Mathematically, this can be formulated as follows:

$$x_k^{\mathrm{IO}} = \max(0, L_k - g_{k+1}) \qquad k : 1, 2, \ldots, n_K, \tag{10}$$

$$g_k = \max(0, g_{k+1} - L_k) \qquad k : 1, 2, \ldots, n_K, \tag{11}$$

$$g_{n_K+1} = p^{\mathrm{pv}} + p^{\mathrm{w}} + p^{\mathrm{de}}, \tag{12}$$

$x_k^{\mathbf{IO}}$: Interrupted load of level k,

g_k : Remaining power after supplying load demand of level k,

L_k : Load value of level k.

n_K : Number of load segments.

Note that x_k^{IO} actually stands for $x_{m,t,k,\omega}^{\mathrm{IO}}$; for readability, the running indices of MGs, time intervals, and scenarios have been removed in these equations.

4.4. Loss of load during joint operation

When a number of MGs operate together, they can assist each other to minimise the interruption costs. However, the ownership of MGs is an important aspect here. If all MGs have the same owner, the only goal is to minimise the total interruption cost and there is no difference in interruption of load points with the same interruption cost in any of the MGs. In this case, a method similar to the one utilised for island mode can be considered for calculating the interrupted load by aggregating the generation and loads (with the same interruption cost) of all MGs. However, when MGs have different owners and are self-interested, each MG seeks to supply its own load first and then sell its excess energy to the other ones. On the other hand, since the interruption cost of all load points is not the same, a seller MG might interrupt its loads with lesser interruption cost and sell it to a buyer that wants to supply a load with a higher interruption cost. Although applying an appropriate pricing mechanism will benefit both parties, the conventional reliability indices, such as EENS, consider this interrupted load of the seller as the energy not supplied for this MG. In this regard, two indices—Interrupted but Gained Compensation (IbGC), and Supplied by Expensive Resources (SbER)—that we have recently proposed for self-interested MMGs [12], are calculated besides EENS.

When MGs are in joint operation, there might be more than one seller or buyer with similar conditions but limited buying or selling requests, respectively. By way of illustration, assume that the sellers have 1 MW excess power in total but there are two buyers with 1 and 1.5 MW of power requests. The problem is how to share the power between the MGs. We have used the *'bankruptcy problem'* [15] which is the division of insufficient resources—energy deficit/excess— between the claimants—buyers/sellers. This method is based on the game theory concepts, and it has been used for the same purpose in the field of power systems [16] but for loads with the same interruption cost and only for the cases where there is energy deficit in the system. In this study, the method has been extended to include loads with interruption costs for different load sectors and both energy deficit and energy surplus.

The procedure for calculating the transactions between MGs is elaborated in the following. Note that, for readability, the indices of joint operations j, generation-load scenarios ω, and time intervals t have been removed. Suppose that $\mathcal{M}^{\mathrm{JO}}$ is the set of MGs participating in joint operation. Let the negative values of $\mathcal{P}_m$ be the available power of seller MGs, and its positive values be the requested power of buyer MGs. Let $\beta = \mathrm{sgn}\left(\sum_{m\in\mathcal{M}^{\mathrm{JO}}} \mathcal{P}_m\right)$, where sgn is the sign function. Then $\beta = -1$ indicates a surplus of available power, $\beta = 1$ indicates a deficit in available power, and $\beta = 0$ indicates the balance between the available and requested power. The transactions between the MGs is then calculated using different rules of '*bankruptcy problem*', including: Equal Shares (ES), Equal Shares of Deficit (ESoD), and Proportional Shares (PS), as follows:

$$\text{ES:} \begin{cases} \sum_{m\in\mathcal{M}'} \min\left(\beta\cdot\mathcal{P}_m, \psi\right) = \sum_{m\in\mathcal{M}_t''} |\mathcal{P}_m| \\ \mathcal{P}_m^* = \beta\cdot\min\left(\beta\cdot\mathcal{P}_m, \psi\right) \qquad : \forall_m \in \mathcal{M}_t' \end{cases} \tag{13}$$

$$\text{ESoD:} \begin{cases} \sum_{m\in\mathcal{M}_t'} \max\left(0, \beta\cdot\mathcal{P}_m - \psi\right) = \sum_{m\in\mathcal{M}_t''} |\mathcal{P}_m| \\ \mathcal{P}_m^* = \beta\cdot\max\left(0, \beta\cdot\mathcal{P}_m - \psi\right) \qquad : \forall_m \in \mathcal{M}_t' \end{cases} \tag{14}$$

$$\text{PS:} \begin{cases} \psi = \frac{\sum_{m\in\mathcal{M}_t''} |\mathcal{P}_m|}{\sum_{m\in\mathcal{M}_t'} |\mathcal{P}_m|} \\ \mathcal{P}_m^* = \mathcal{P}_m\cdot\psi \qquad : \forall_m \in \mathcal{M}_t' \end{cases} \tag{15}$$

where $\mathcal{M}' = \left\{m | m \in \mathcal{M}^{\mathrm{JO}}, \beta\cdot\mathcal{P}_m \geq 0\right\}$ and $\mathcal{M}''$ indicates its complement w.r.t. $\mathcal{M}^{\mathrm{JO}}$. For each of the employed rules, solving the first equation gives ψ which is then used to obtain $\mathcal{P}_m^*$. Note that $\mathcal{P}_m^* = \mathcal{P}_m : \forall_m \in \mathcal{M}''$. Algorithm 2 settles the exchanged power between the MGs based on one of the above rules, and accordingly, calculates the interrupted load for each scenario of generation-load at each time interval during a joint operation. The input to this algorithm is a scenario that includes the generation of DGs together with load demand of all load segments (generation-load) of the MGs involved in the joint operation ($\mathcal{M}^{\mathrm{JO}}$). The positive value of g_k^{tot} is the total remaining power after supplying load level k of all MGs in joint operation mode. Based on this algorithm, the load interruption occurs at the load level k, where g_k^{tot} is less than zero. This is checked using the condition in line 18 of Algorithm 2. If g_k^{tot} is positive at the load level k, but some MGs face energy deficit ($d_m > 0$) at this load level (which is checked through the condition in line 6), the seller and buyer MGs trade based on one of the aforementioned rules. The exchanged power ($\mathbf{p}^{\mathrm{ex}}$) and the interrupted loads ($x_{m,k}^{\mathrm{JO}}$) are the output of this algorithm and are then used to calculate the EENS, IbGC, and SbER indices. The procedure for the calculation of IbGC and SbER indices has been explained in [12]. Note that the positive value of $\mathbf{p}^{\mathrm{ex}}$ yields the purchased power.

Algorithm 2: Calculate the adequacy indices for MGs in joint operation mode in a specific generation-load scenario.

Input : Generation-load.

Output: $x^{\mathrm{JO}}_{m,k}$: $\forall_m \in \mathcal{M}^{\mathrm{JO}}, \forall_k \in \{1:n_K\}$; $\mathbf{p}^{\mathrm{ex}}$.

Calculate $g_{m,k} \leftarrow p^{\mathrm{pv}}_m + p^{\mathrm{w}}_m + p^{\mathrm{de}}_m - \sum_{k'=k}^{n_K} L_{m,k'}$: $\forall_m \in \mathcal{M}^{\mathrm{JO}}$, $\forall_k \in \{1:n_K\}$;

Calculate $g^{\mathrm{tot}}_k \leftarrow \sum_{m\in\mathcal{M}^{\mathrm{JO}}} g_{m,k}$ $\forall_k \in \{1:n_K\}$;

$\mathbf{p}^{\mathrm{ex}} \leftarrow \mathbf{0}^{n_m\times 1}$ (exchanged power);

for $k_1 \leftarrow n_K$ **to** 1 **step** -1 **do**

  $d_m \leftarrow -g_{m,k_1} - p^{\mathrm{ex}}_m \quad \forall_m \in \mathcal{M}^{\mathrm{JO}}$;

  if $g^{\mathrm{tot}}_{k_1} > 0$ & *d_m is positive for at least one MG* **then**

    Find set of seller ($\mathcal{M}^{\mathrm{s}}$) and buyer ($\mathcal{M}^{\mathrm{b}}$) MGs;

    $k_2 = 1$;

    while $d_m \neq 0$: $\forall_m \in \mathcal{M}^{\mathrm{b}}$ **do**

      $\mathcal{P}_m \leftarrow d_m : \forall_m \in \mathcal{M}^{\mathrm{b}}$;

      $\mathcal{P}_m \leftarrow -g_{m,k_2} - p^{\mathrm{ex}}_m : \forall_m \in \mathcal{M}^{\mathrm{s}}$;

      $\mathcal{P}_m \leftarrow 0 : \forall_m \in \mathcal{M}^{\mathrm{s}}$ & $-g_{m,k_2} - p^{\mathrm{ex}}_m \geq 0$;

      $\boldsymbol{\mathcal{P}}^* \leftarrow EqualShares(\boldsymbol{\mathcal{P}})$;

      $\mathbf{d} \leftarrow \mathbf{d} - \boldsymbol{\mathcal{P}}^*$;

      $\mathbf{p}^{\mathrm{ex}} \leftarrow \mathbf{p}^{\mathrm{ex}} + \boldsymbol{\mathcal{P}}^*$;

      $k_2 \leftarrow k_2 + 1$;

    end

  else if $g^{\mathrm{tot}}_{k_1} <= 0$ **then**

    if $d_m >= 0$ $\forall_m \in \mathcal{M}^{\mathrm{JO}}$ **then**

      $x^{\mathrm{JO}}_{m,k_1} \leftarrow d_m : \forall_m \in \mathcal{M}^{\mathrm{JO}}$;

    else

      $\boldsymbol{\mathcal{P}} \leftarrow \mathbf{d}$;

      $\boldsymbol{\mathcal{P}}^* \leftarrow EqualShares(\boldsymbol{\mathcal{P}})$;

      $\mathbf{p}^{\mathrm{ex}} \leftarrow \mathbf{p}^{\mathrm{ex}} + \boldsymbol{\mathcal{P}}^*$;

      $x^{\mathrm{JO}}_{m,k_1} \leftarrow d_m - \mathcal{P}^*_m : \forall_m \in \mathcal{M}^{\mathrm{JO}}$;

    end

    $x^{\mathrm{JO}}_{m,k} \leftarrow L_{m,k} : \forall_m \in \mathcal{M}^{\mathrm{JO}}$ & $\forall_k \in \{1:k_1-1\}$;

    Stop the program;

  end

end

The bold font of a variable denotes a column vector $\forall_m \in \mathcal{M}^{\mathrm{JO}}$.

4.5. Impact of failure of third category of components

The impact of third category of components has not yet been incorporated into the model. First, note that these components only affect the adequacy indices during island and joint modes. The probability of failure of these components during a contingency—islanding or joint—is generally very low and, as it will be shown in the result, it makes a negligible impact on the adequacy indices. However, it places a great computational burden on the model. Accordingly, it can be totally disregarded if computational time is the main determinant; otherwise, in cases that the accuracy of the model is the main determinant, considering a single failure at a time for the contingencies with higher probability would suffice. In addition, note that the simulation-based methods also require an enormous number of samples to capture these impacts.

A set of events and their corresponding probabilities are specified to incorporate the impact of these components. Let $\mathcal{I}$ be the set of operation modes (islanding & joint) that are of interest to incorporate the impact of third category of components on them. Let $\mathcal{O}^E_i$ be the components in the third category whose single failure affects the DGs and loads in operation mode $i \in \mathcal{I}$. For the cyber structure in Fig. 1, these components are LCs, MCs, and SWs at each of the buses, and the cyber links between them; the cyber link between the SW of each bus and MGCC; transformers; and DGs. The failure of these components results in either load interruption, uncontrollable load points, or outage of generation units. The probability of single failures can be derived using Equation (1) in which only one component fails at a time. The events with the same consequence are then aggregated as one event by summing their probabilities. Let $\{\Lambda_i\}_{i\in\mathcal{I}} = \{\lambda|\lambda = 1 : n^{\Lambda}_i\}$ be a family of sets, where Λ_i and n^{Λ}_i are the set and number of events for operation mode i, respectively; Accordingly, the failed DGs $\mathcal{F}^{\mathrm{g}}_{i,\lambda}$, interrupted load points $\mathcal{F}^{\mathrm{l}}_{i,\lambda}$, uncontrollable load points $\mathcal{F}^{\mathrm{lc}}_{i,\lambda}$, and probability of occurrence $\rho^{\Lambda}_{i,\lambda}$ of event λ in operation mode i can be determined. Another event, in which there is no failure, is added to each set Λ_i with the probability of $\rho^{\Lambda_i}_{\lambda+1} = 1 - \sum_{1:n^{\Lambda}_i} \rho^{\Lambda}_{i,\lambda}$. We can now incorporate the impact of this set of events on each of the scenarios at each time interval for operation mode i.

5. Calculating adequacy indices

The overall EENS for each MG m at each load segment k is equal to the summation of the EENS in various operation modes as follows:

$$\mathrm{EENS}_{m,k} = \mathbf{EENS^{GC}_{m,k}} + \mathbf{EENS^{JO}_{m,k}} + \mathbf{EENS^{IO}_{m,k}} + \mathbf{EENS^{SD}_{m,k}}. \tag{16}$$

During the normal operation, with the support of upstream grid, no load shedding occurs as a result of energy deficit. The only cause of interrupted loads in this case is the outage of the loads themselves. The failure of transformers, in this study, is the only source of this type of failure. Therefore, we have:

$$\mathbf{EENS^{GC}_{m,k}} = \rho^{\mathrm{GC}}_m \times U^{\mathrm{tr}} \times \sum_{t\in\mathcal{T}} h_t \times L_{m,k,t} \ , \tag{17}$$

where, ρ^{GC}_m is the probability that MG m is in normal operation mode; $\mathcal{T}$ is the set of time intervals; h_t is the number of hours that time interval t represents; U^{tr} is the unavailability of transformers; and $L_{m,k,t}$ is the load demand of microgrid m at load segment k and time interval t.

During the shutdown mode, all the local generation resources shut down, and all loads are interrupted; therefore, we have:

$$\mathbf{EENS^{SD}_{m,k}} = \rho^{\mathrm{SD}}_m \times \sum_{t\in\mathcal{T}} h_t \times L_{m,k,t} \ , \tag{18}$$

where, ρ^{SD}_m is the probability that MG m is in shutdown mode.

During the islanding mode, the EENS is calculated w.r.t. the generation level of renewable generation resources as follows:

$$\mathbf{EENS^{IO}_{m,k}} = \rho^{\mathrm{IO}}_m \times \sum_{t\in\mathcal{T}} h_t \times \sum_{\omega\in\Omega_t} \rho^{\Omega}_{\omega,t} \times x^{\mathrm{IO}}_{m,t,k,\omega}. \tag{19}$$

where $x^{\mathrm{IO}}_{m,t,k,\omega}$ is calculated using (10)–(12). $\rho^{\Omega}_{\omega,t}$ yields the probability of scenario ω of generation-load at time period t.

Each MG might participate in more than one combination of joint operation mode with a certain probability. Let J be the set of possible combinations of joint operation mode, and $\{\mathcal{M}^{\mathrm{JO}}_j\}_{j\in J}$ be a family of sets, where $\mathcal{M}^{\mathrm{JO}}_j$ is the set of MGs that participate in combination j of joint operation with its associated occurrence probability ρ^{JO}_j. Then we have:

$$\mathbf{EENS^{JO}_{m,k}} = \sum_{j|m\in\mathcal{M}^{\mathrm{JO}}_j} \rho^{\mathrm{JO}}_j \times \sum_{t\in\mathcal{T}} h_t \times \sum_{\omega\in\Omega_t} \rho^{\Omega}_{\omega,t} \times x^{\mathrm{JO}}_{m,t,k,\omega,j}. \tag{20}$$

where $x^{\mathrm{JO}}_{m,t,k,\omega,j}$ is the interrupted load of microgrid m at time period t, load segment k, generation-load scenario ω, and during joint operation j which is obtained using Algorithm 2.

6. Results

All the simulations were conducted in MATLAB 2021b. For those results where computational times have been reported, a Windows based personal computer with Intel CORE i7 processors clocking at 2.8 GHz and 32 GB of RAM were used. Note that MATLAB Coder has

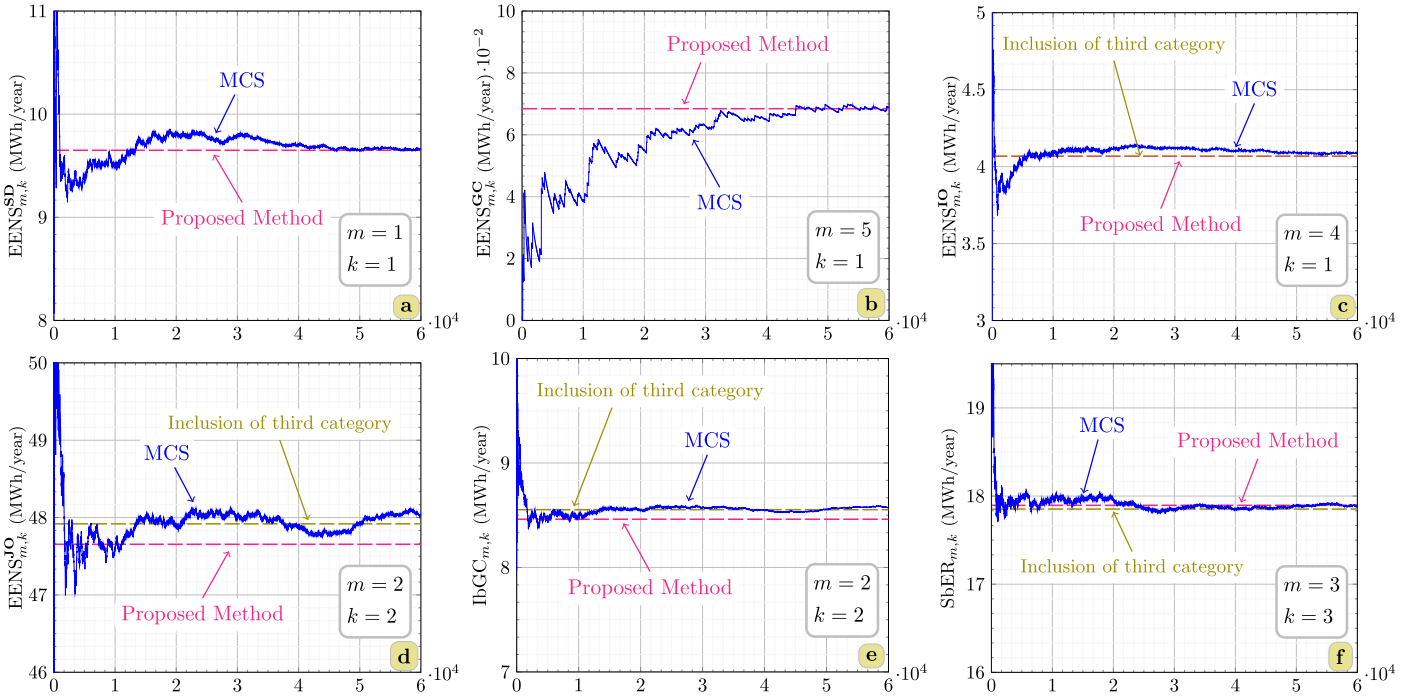

Fig. 5. The result of the proposed approach versus MCS. The horizontal axes shows the number of samples of simulation years in all figures. m and k yields the associated MG and load segment, respectively. For instance, (a) indicates $EENS^{SD}_{1,1}$, which is the contribution of shut down mode to the EENS adequacy index for MG #1 and load segment #1 (residential loads).

Table 2
Capacity of distributed generation in each MG.

Parameters	(unit)	Microgrids				
		1	2	3	4	5
P^{w}	(MW)	0.5	1.1	1	0.6	0.5
P^{pv}	(MW)	1	0.6	1.6	0	1.6
P^{de}	(MW)	0.7	0.4	0	0.6	0.8

Table 3
Type of load points.

Load type	Load points
Residential	1, 4, 6, 9, 11, 14, 16, 19, 22
Commercial	2, 5, 7, 10, 12, 17, 20, 23
Industrial	3, 8, 13, 15, 18 , 21

been used to build MEX[1] (MATLAB executable) files for Algorithms 1 and 2 for both the proposed and MCS-based methods.

6.1. Case study

Feeder 4 at bus 6 of Roy Billinton Test System (RBTS) distribution network presented in [17] has been considered as a base case, and it has been extended to form a CPMMG by adding DGs and cyber infrastructure as shown in Fig. 1. Table 2 shows the capacity of the added DGs. Detailed data for the distribution system can be found in [17], except for the load types that have been changed to include different load sectors in the CPPMG; Table 3 indicates the type of loads at each load point, in which interruption cost increases from the top row to the bottom row. The failure and repair rates can be found in [11], except for the DGs. The mean time to failure and repair of DGs are 5000 and 10 h, respectively.

[1] A MEX file is a function, created in MATLAB, that calls a C/C++ program or a Fortran subroutine. A MEX function behaves just like a MATLAB script or function.

6.2. Validation of the proposed method vs. MCS

Fig. 5 shows the results obtained by both the proposed and MCS-based methods for a few different modes, MGs, and load segments. The result conclusively proves the ability of the proposed approach in calculating the adequacy of CPMMGs. Fig. 5.a-d show the contribution of various operation modes to the EENS adequacy index. For instance, 5.c indicates the contribution of the islanding operation mode to the EENS adequacy index in MG #4 and for residential sector ($k = 1$). The inclusion of the third category of components only impacts the joint and islanding operation modes. Since it influences the joint operation mode, it has an impact on IbGC and SbER adequacy indices accordingly. As can be seen from this figure, the impact of failure of third category of components is very small. Note that for the results indicated by *"proposed method"* in Fig. 5, setting **S2** (defined in section 6.4.1) has been used.

6.3. Analysing the duration of operation modes

Table 4 shows the probability of various operation modes with ideal and non-ideal cyber systems. A key observation in this table is that the cyber failures mostly affect the island & shutdown modes, due to the failure of DMS and MGCC, respectively. The dominant components of cyber system, w.r.t. their impact on adequacy indices, are therefore the main controllers, viz., DMS and MGCCs. In addition, the first and second rows of joint operation mode exert a major impact on the loss of load. Therefore, presence of a backup supply connected to either of MGs #2, #3, #4, or #5 will drastically decrease the loss of load in the system.

6.4. Computational time vs. accuracy & scalability

In order to calculate the error of the case studies and for further analysis, first, a case using MCS method with a vast number of sample years (1.2×10^6) has been simulated, and the results have been considered as a basis.

Table 4
Various plausible operation modes together with their occurrence probability and duration.

Operation mode	List of microgrids	Non-ideal cyber system		Ideal cyber system	
		Prob.*	Duration [h/year]	Prob.*	Duration [h/year]
Joint mode	1, 2, 3, 4, 5	1.07e−02	93.77	1.06e−02	93.14
	2, 3, 4, 5	1.38e−03	12.13	8.94e−04	7.83
	1, 2, 3, 4	2.06e−05	0.18	1.53e−05	0.13
	1, 2, 4, 5	2.02e−05	0.18	1.48e−05	0.13
	1, 2, 3, 5	1.47e−05	0.13	9.41e−06	0.08
	2, 3, 4	2.63e−06	0.02	1.27e−06	0.01
	2, 4, 5	2.58e−06	0.02	1.23e−06	0.01
	2, 3, 5	1.87e−06	0.02	7.83e−07	0.00
Island mode	1	5.16e−04	4.52	1.81e−05	0.16
	2	4.92e−04	4.31	0	0.00
	3	2.68e−03	23.50	1.70e−03	14.89
	4	2.68e−03	23.52	1.70e−03	14.89
	5	2.68e−03	23.51	1.70e−03	14.89
Shutdown mode	1	1.35e−03	11.83	8.53e−04	7.47
	2	2.15e−03	18.85	1.66e−03	14.51
	3	1.84e−03	16.12	1.34e−03	11.79
	4	1.33e−03	16.67	8.38e−04	7.34
	5	1.88e−03	16.51	1.39e−03	12.18

The probability of being in normal operation mode for each of MGs is equal to prob(normal) = 1 - prob(islanding OR joint OR shutdown modes). For example, the probability that MG #1 is in normal operation mode is equal to 1 − 0.0005 − 0.0108 − 0.0014 = 0.987.
*Prob. stands for probability of occurrence.

6.4.1. Options for trade-offs between the computational time and accuracy

In the proposed method, the options listed below provide a trade-off between the accuracy and the computational time.

(1) Threshold of the occurrence probability for filtering the negligible contingencies in the SEM. (σ_1).
(2) Threshold of the occurrence probability for filtering the insignificant contingencies of switches in mis-operation mode (σ_2).
(3) Number of the intervals considered for the PDFs representing the hourly wind speed and solar radiation (n^{w} and n^{pv}).
(4) Threshold of the occurrence probability for filtering the less likely joint and island operation modes (σ_3).
(5) The inclusion or omission of the third category of the components in the model.

The computational time of the proposed method includes two main parts: the time required for determining different operation modes and their probability of occurrence, and the time required for calculating the indices for each of these operation modes. Options #1 and #2 of the aforementioned list influence the first part, and options #3–5 impact the second part. To exemplify the impact of each of these options, Table 5 reports the computational time for the proposed method with the settings **S1–S5** outlined below.

	Third category	n^{pv}	n^{w}	σ_1	σ_2	σ_3
S1:	✓	10	10	0	$3e-5$	0
S2:	✗	10	10	0	$3e-5$	0
S3:	✗	10	10	$1e-7$	$3e-5$	0
S4:	✗	10	10	$1e-7$	$3e-5$	$1e-4$
S5:	✗	6	6	$1e-7$	$3e-4$	$1e-4$

The computational time of the proposed approach, as can be seen in Table 5, depends largely on the evaluation of the third category of components; however, it has a limited impact on the adequacy indices, and disregarding them results in a minor error (0.18%). By filtering the insignificant contingencies from the state space generated by SEM, as in **S3**, the computational time decreases slightly while the error barely increases. Although this option slightly improves the computational time in this case, as will be revealed afterwards, it is crucial when the system scales. Another option is neglecting the operation modes with a negligible probability of occurrence. As can be seen in Table 4, the occurrence probability for most of the combinations of MGs in joint operation mode is extremely low. Disregarding these modes improves the speed of the computation. Fewer number of intervals for the segmentation of PDFs associated with RERs, as has been considered in **S5**, will further accelerate the computation with the error still less than 1% (0.87%). It is worth mentioning that this option can be chosen variably. For instance, a smart choice would be to choose different number of PDF intervals w.r.t the occurrence probability of the operation modes. Another smart choice would be to choose σ_2 variably with respect to the probability of the states (produced by SEM). This will improve the computational time without sacrificing the accuracy. For illustration, more PDF intervals for the first joint mode in Table 4 can be considered. The computational time of the MCS-based approach depends on the number of sample years and, therefore, on the stopping criterion. Note that no effort was expended to reduce the computational time of the MCS-based method. It is worth mentioning that the error has been calculated as in (21).

Table 5
Computational time of the proposed method vs. MCS.

Method	Settings	Computational time [s]	Error [%]
Proposed approach	**S1**	8.6[a]	0.22%
	S2	0.96[a]	0.40%
	S3	0.81[a]	0.44%
	S4	0.48[a]	0.72%
	S5	**0.29**[a]	0.87%
MCS	6×10^4 sample years	1800	Mean = 0.23%, std. = 0.17[b]

[a]The average time of 100 runs.
[b]The mean and standard deviation for percentage of error of 12 runs.

$$\text{Error} = \frac{\sum_m \sum_r \left|\text{EENS}_{m,r} - \text{EENS}_{m,r}^{\text{base}}\right|}{\sum_m \sum_r \text{EENS}_{m,r}^{\text{base}}} \times 100. \tag{21}$$

6.4.2. Relative error & computational time vs. the number of PDF intervals

Since the segmentation of the PDFs that characterise volatile RERs is extensively used in adequacy assessment, this section further reveals the impact of number of PDF intervals on the accuracy of the overall EENS adequacy index. Setting **S2** has been taken into account for this study. A case with $n^{w} = 50$ and $n^{pv} = 50$ has been considered as the basis for calculating relative errors. Fig. 6.a depicts the relative error

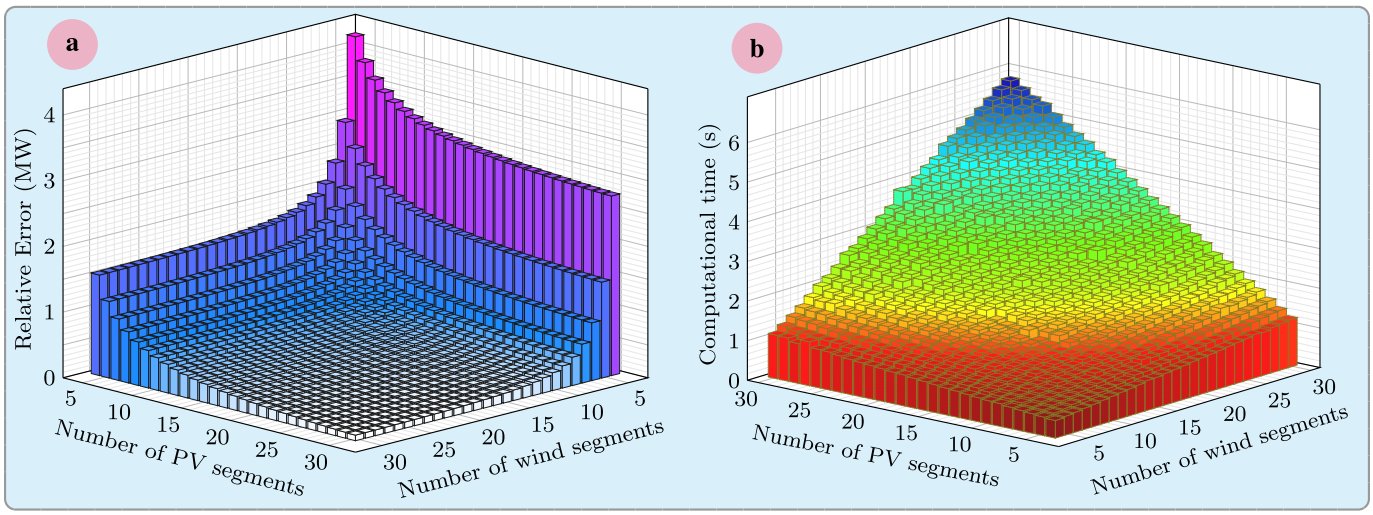

Fig. 6. (a) Relative error versus the number of intervals for wind speed and solar radiation PDFs; and (b) Corresponding computational time.

of the system's EENS w.r.t. the base case ($n^{w} = 50$ and $n^{pv} = 50$), and Fig. 6.b indicates their corresponding computational time. Less than four segments result in a major error and has not been shown in these figures. In addition, by increasing the number of intervals to six for wind speed, the error rather decreases.

6.4.3. Does N-1 contingency suffice for adequacy assessment?

As mentioned in Section 3.3, using SEM, it can be easily checked whether a higher order of contingency is required for the adequacy assessment. In the system under study, the probability of (N-1), (N-2), and any higher order of contingencies are $2.04e-02$ (178.8 h/year), $1.5e-04$ (1.31 h/year), and $6.12e-07$ (5.2e−03 h/year), respectively, for the components of the first category. Obviously, the impact of the contingencies with three or more simultaneous failures is absolutely negligible. Although these numbers depend on both the system topology, and the failure and repair rates of the components, considering only the first order contingencies gives a reasonable approximation of the system adequacy.

6.4.4. Scalability

Increase in the system's scale results in an exponential growth in both the state space of SEM and the number of combinations for the joint operation mode. The solution for the first problem is to filter the states with negligible occurrence probability. In addition, most of the combinations for joint operation modes have an insignificant occurrence probability and can be easily disregarded without causing major error, which solves the second problem. By placing six more power switches between buses 2–3, 8–9, 11–12, 15–16, 17–18, and 21–22 the system scales to 11 MGs. With the settings **S2–S5**, the computational times were 9.8, 3.7, 1.4, and 0.8 seconds, respectively. By decreasing the threshold that filters the SEM output, the computation can be further accelerated, just with slight error. Most of the analytical approaches take single contingencies (N-1 criteria) into account for the calculation of adequacy indices. These contingencies as explained in Section 6.4.3 are the major cause of load interruption. Therefore, the proposed approach will pass the scalability test. It is also worth mentioning that parallel computing can be used for both the MCS-based approach and the proposed approach.

7. Concluding remarks

In this paper, a novel analytical approach for obtaining the EENS adequacy index in a CPMMG has been proposed, and validated against a simulation-based approach. The proposed analytical method illustrated that through the incorporation of the unique characteristics of a CPMMG into the modelling and the classification of components into unique categories, it is viable to decrease the computational time for acquiring the adequacy indices in CPMMG systems. It has also been shown that the aggregation of components does not sacrifice the accuracy, and yet offers a favourable opportunity to include a desirable degree of system's detail. In addition, the model is capable of filtering negligible contingencies for an even faster problem solving. Two useful directions for the future work based on this research study from the perspective of power and cyber systems could be the inclusion of energy storage systems into the distribution system and designing the cyber system based on 5G technologies.

CRediT authorship contribution statement

Mostafa Barani: Conceptualization, Methodology, Software, Writing – original draft, Data curation. **Vijay Venu Vadlamudi:** Supervision, Writing – review & editing, Funding acquisition.

Declaration of competing interest

The authors declare that they have no known competing financial interests or personal relationships that could have appeared to influence the work reported in this paper.

Acknowledgments

This work was originally funded and supported by NTNU Energy (Project No. 81770920), which is gratefully acknowledged. The corresponding author also gratefully acknowledges the partial extended financial support from the ERA-Net SES & Research Council of Norway through the project HONOR (Project No. 309146).

References

[1] E.J. Ng, R.A. El-Shatshat, Multi-microgrid control systems (MMCS), in: IEEE PES General Meeting, 2010, pp. 1–6.
[2] S.A. Arefifar, Y.A.-R.I. Mohamed, T. El-Fouly, Optimized multiple microgrid-based clustering of active distribution systems considering communication and control requirements, IEEE Trans. Ind. Electron. 62 (2) (2015) 711–723.
[3] R.H. Lasseter, Smart distribution: Coupled microgrids, Proc. IEEE 99 (6) (2011) 1074–1082.
[4] B. Falahati, Y. Fu, L. Wu, Reliability assessment of smart grid considering direct cyber-power interdependencies, IEEE Trans. Smart Grid 3 (3) (2012) 1515–1524.
[5] I.A. Tøndel, J. Foros, S.S. Kilskar, P. Hokstad, M.G. Jaatun, Interdependencies and reliability in the combined ICT and power system: An overview of current research, Appl. Comput. Inform. 14 (1) (2018) 17–27.

[6] B. Falahati, Y. Fu, Reliability assessment of smart grids considering indirect cyber-power interdependencies, IEEE Trans. Smart Grid 5 (4) (2014) 1677–1685.
[7] W. Liu, Q. Gong, H. Han, Z. Wang, L. Wang, Reliability modeling and evaluation of active cyber physical distribution system, IEEE Trans. Power Syst. 33 (6) (2018) 7096–7108.
[8] W. Liu, Z. Lin, L. Wang, Z. Wang, H. Wang, Q. Gong, Analytical reliability evaluation of active distribution systems considering information link failures, IEEE Trans. Power Syst. 35 (6) (2020) 4167–4179.
[9] C. Wang, T. Zhang, F. Luo, F. Li, Y. Liu, Impacts of cyber system on microgrid operational reliability, IEEE Trans. Smart Grid 10 (1) (2019) 105–115.
[10] H. Farzin, R. Ghorani, M. Fotuhi-Firuzabad, M. Moeini-Aghtaie, A market mechanism to quantify emergency energy transactions value in a multi-microgrid system, IEEE Trans. Sustain. Energy 10 (1) (2019) 426–437.
[11] M. Barani, V.V. Vadlamudi, P.E. Heegaard, Reliability analysis of cyber-physical microgrids: Study of grid-connected microgrids with communication-based control systems, IET Gener. Transm. Distrib. 15 (4) (2021) 645–663.
[12] M. Barani, V.V. Vadlamudi, H. Farzin, Impact of cyber failures on operation and adequacy of multi-microgrid distribution systems, 2022, arXiv:2204.08526 [eess.SY].
[13] Y.M. Atwa, E.F. El-Saadany, M.M.A. Salama, R. Seethapathy, Optimal renewable resources mix for distribution system energy loss minimization, IEEE Trans. Power Syst. 25 (1) (2010) 360–370.
[14] P.J. Balducci, J.M. Roop, L.A. Schienbein, J.G. DeSteese, M.R. Weimar, Electric Power Interruption Cost Estimates for Individual Industries, Sectors, and U.S. Economy, Pacific Northwest National Laboratory Report, Feb. 2002.
[15] W. Thomson, Axiomatic and game-theoretic analysis of bankruptcy and taxation problems: a survey, Math. Social Sci. 45 (3) (2003) 249–297.
[16] H. Farzin, M. Fotuhi-Firuzabad, M. Moeini-Aghtaie, Reliability studies of modern distribution systems integrated with renewable generation and parking lots, IEEE Trans. Sustain. Energy 8 (1) (2017) 431–440.
[17] R. Billinton, S. Jonnavithula, A test system for teaching overall power system reliability assessment, IEEE Trans. Power Syst. 11 (4) (1996) 1670–1676.